02 Nov 2020

Explosive Compaction of Additively Manufactured Material

Phillip R. Mulligan
Missouri University of Science and Technology, pmulligan@mst.edu

Cody Lough

Douglas A. Bristow
Missouri University of Science and Technology, dbristow@mst.edu

Edward Kinzel

et. al. For a complete list of authors, see https://scholarsmine.mst.edu/mec_aereng_facwork/4588

Recommended Citation

P. R. Mulligan et al., "Explosive Compaction of Additively Manufactured Material," *AIP Conference Proceedings*, vol. 2272, article no. 110008, American Institute of Physics (AIP), Nov 2020.
The definitive version is available at https://doi.org/10.1063/12.0000847

Explosive Compaction of Additively Manufactured Material

Phillip Mulligan[1,*], Cody Lough[1], Douglas Bristow[1], Edward Kinzel[2], and Catherine Johnson[1]

[1]*Missouri University of Science and Technology, 1006 Kingshighway, Rolla, MO, 65409, USA*
[2]*University of Notre Dame, Notre Dame, IN 46556, USA*

[*]*Corresponding author: pmulligan@mst.edu*

Abstract. Selective Laser Melting (SLM) is an additive manufacturing (AM) technique that uses a laser to locally fuse material in a metal-powder bed. The process is performed in layers enabling significant geometric freedom over traditional manufacturing techniques. During the deposition process, the metal is locally melted and rapidly self-quenched, leading to rapid solidification with well-defined melt-pool boundaries. Analogies are often drawn to the microstructure created in welding, albeit extending to the entire part. The SLM process parameters are optimized to produce near full density metal parts. The process parameters can also be adjusted to produce local regions that are of unmelted or partially melted powders. The ability to tailor the density (and corresponding modulus, yield strength, and ductility) continuously on a volumetric basis, has significant potential to engineer effective properties. This paper reports on an experimental study of AM metal components subjected to dynamic loading by detonating an explosive in intimate contact with the material. The crystallographic structural behavior of the parts is characterized before and after explosive loading in an explosive compaction test. The findings will aid in designing AM components for explosively loaded systems.

INTRODUCTION

Previous studies have utilized Selective Laser Melting (SLM) to create Additively Manufactured (AM) metal parts that are exposed to explosive loading [1, 2, 3]. These experiments indicated that the SLM parts are undergoing a different failure process than the same part produced with traditional manufacturing techniques, such as CNC machining of cold-rolled metal. This motivates a closer examination of how the material fails under explosive loading is needed to recognize SLM's potential in explosive systems fully. A better understanding how SLM created materials respond under dynamic loading will aid in designing components that maximize the performance in explosively loaded systems, which is significant because the versatility of the SLM process is beneficial for several explosive loading scenarios. The research presented in this paper focuses on inducing failure in three different states of 304L stainless steel. Stainless steel was chosen based on prior experience processing the material with SLM at Missouri S&T. Each state of stainless steel is exposed to an explosively driven compressive load that exceeds the ultimate yield and tensile strength of the stainless steel cores.

BACKGROUND

Explosive compaction is often used for material model development and characterizing material behavior in extreme conditions. During a typical explosive compaction study, an annulus is made to house the sample material [4]. The annulus typically has a waveshaper or cone at the top that forces the shock wave to apply a radially compressive force as the shock wave travels along the axis of the annulus. The compressive force applied can bond un-compacted powder into a billet or induce the failure of a material. The radial shock wave traveling through the material collides along the center axis of the annulus, resulting in a significant spike of the peak pressure [5]. As the compressive force associated with the converging shock wave releases, a tensile force is produced [6, 7]. Producing a billet from powdered material is a difficult process requiring uniform powder material, near-perfect axisymmetric

Shock Compression of Condensed Matter - 2019
AIP Conf. Proc. 2272, 110008-1–110008-5; https://doi.org/10.1063/12.0000847
Published by AIP Publishing. 978-0-7354-4000-5/$30.00

loading, and a tight tolerance on the compressive forces applied to the powder [8]. The experimental procedures presented in this paper are to examine the explosive compaction of SLM created material with a focus on inducing failure.

EXPERIMENTAL PROCEDURE

An annulus configuration was designed from copper to induce failure in the stainless steel cores. The copper annulus consisted of a cone, base, inner pipe, and an outer pipe (see Fig. 1). The stainless steel core was positioned inside the inner pipe, and the components were soldered together. Once the components were soldered together, 315 grams of a 50/50 Comp B mix was poured around the annulus, constrained inside of a polyvinyl chloride (PVC) housing. A soft recovery system was used to collect the annulus and minimize damage to the core that is not associated with the explosive compaction. A standard blasting cap was used to initiate the charge. The estimated compressive force acting on the cores for the annulus design shown in Fig. 1f is 75 GPa. The release force is estimated to be 8 GPa [9, 10]. Three cores were tested for each manufacturing process.

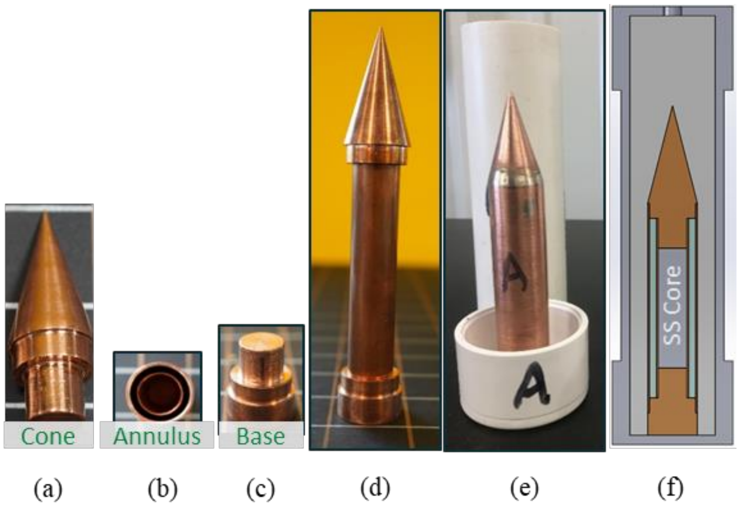

FIGURE 1. Copper annulus Components cone (a), the annulus (b), base (c), and assembly (d, e, and f).

Additive Manufacturing

The SLM process is a powder bed additive manufacturing technique in which 3D metal parts are produced layer by layer. During SLM, a laser scans and fuses the metal powder bed along computer-generated paths defined by the part geometry. The process parameters can be used to control the material's properties [11]. The resulting melt pools generated by the laser fusion of the powder can be seen in Fig. 2. The general appearance is analogues to placoid scales.

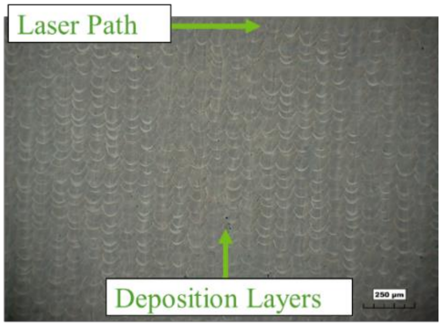

FIGURE 2. An optical micrograph of the cross-sections of laser tracks in SLM created SS 304L, illustrating the molten pool.

The sample in Fig. 2 was mounted in Bakelite, polished to 0.05 μm using a diamond suspension, and then electrolytically etched using 60/40 Nitric acid. For the research presented in this paper, a Renishaw AM250 SLM system was used. The laser power was set to 200 W with an exposure time of 75 μs to produce a high-density AM core (97.5% of the density of the cold-rolled core). The laser power was set to 100 W for 50 μs to produce a lower density AM core (89.9% density of the cold-rolled core). For this research, no post-process treatment was performed on the cores. Figure 3 shows the core material tested during this research.

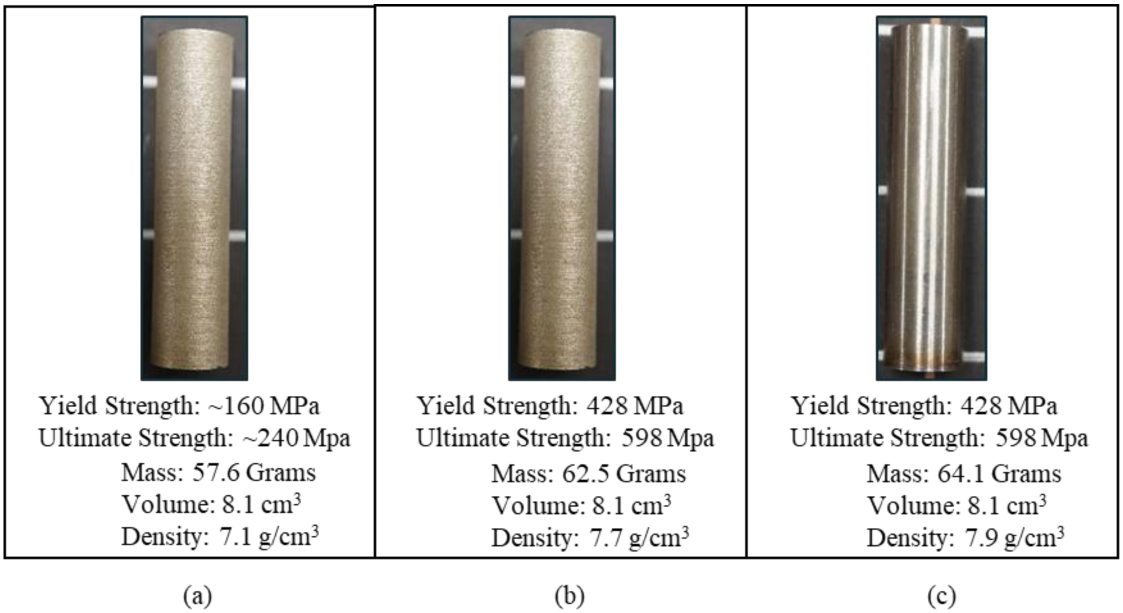

FIGURE 3. Overview of the stainless steel cores with corresponding strength and mass properties: the lower density AM core (a), the higher density AM core (b), and the cold-rolled stainless steel core (c).

While the AM cores appear identical from the exterior of the core, the cross-sections of the cores highlight how cores microstructures differ. Figure 4 shows an electron microscope image of each core. The lower density of the first AM core (Fig. 4a) can be attributed to the porosity produced from the lower laser power and reduced exposure time. The higher density AM core (Fig. 4b) has some porosity, but significantly less than the lower-density AM core. The cold-rolled core has visible worked lines associated with the cold-working process (Fig. 4c).

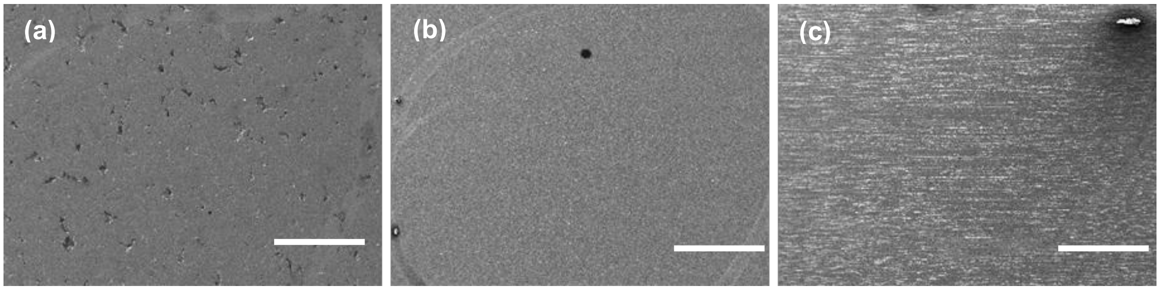

FIGURE 4. Cross-section image of the stainless steel cores at a 1 mm scale.

Further examination of the cores at a higher magnification illustrates the microstructure differences even further. Figure 5 shows a higher magnification electron microscope image of each core. Incompletely melted stainless steel powder can be seen in some of the voids of the lower density AM core, see Fig. 4a. Similar to Fig. 2b, the melt pool boundaries can be seen in Fig 5b. The cold-rolled layers are also more apparent with the increased magnification.

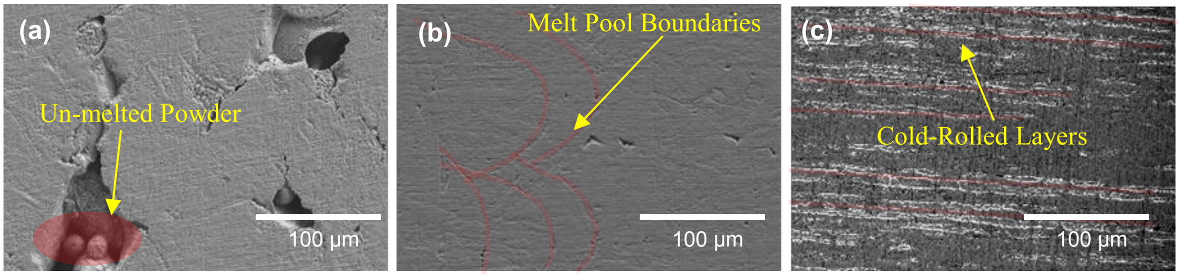

FIGURE 5. Cross-section image of the stainless steel cores at 100 µm scale.

RESULTS

After the explosive compressive test, the lower density printed core broke into five pieces. The largest piece collected was the copper cone. The four smaller pieces make up 65% of the mass of the original core. Note that this mass includes the inner copper pipe. The higher density printed core test remained intact. The annulus lost the copper base. Similarly, the rolled stainless steel core remained primarily intact, although the core appears to have suffered slightly more damage than the high-density printed core.

When a comparison is made of the electron microscope images of each sample, how the microstructures influenced the failure becomes apparent, see Fig 6. It can be seen that the printed cores failed in a granular manner. Whereas, the rolled core appears to have splintered. The lower strength of the lower density AM core resulted in significant failure, Fig. 6a. The voids created impedance mismatches in the material, resulting in spall regions around each void, Fig. 6b. The higher density printed core failed along its center axis, but the failure appears to correspond to the bonding at the melt pool boundaries, see Fig 6c and 6d. With the cold-rolled core, the splintering pattern appears to match the worked lines associated with the rolling process, see Fig. 6e and 6f.

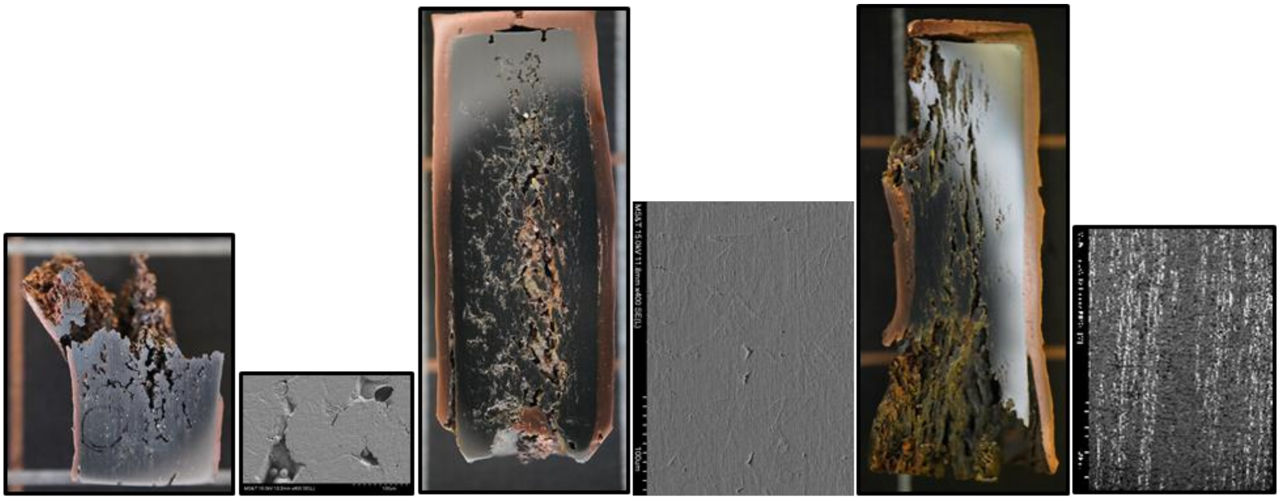

(a) (b) (c) (d) (e) (f)

FIGURE 6. Comparison of how the microstructure of the core, associated with the manufacturing process, influences the core failure under explosive compaction.

Also, of interest is the center of the annulus' cone. In each case, a hollow cavity is generated in the center of the core. The size of the cavity appears to correspond to the failure of the stainless steel core. Upon closer examination, the copper residue is deposited in the failure regions of the stainless steel cores. The copper material appears to be bonded as opposed to loosely deposited.

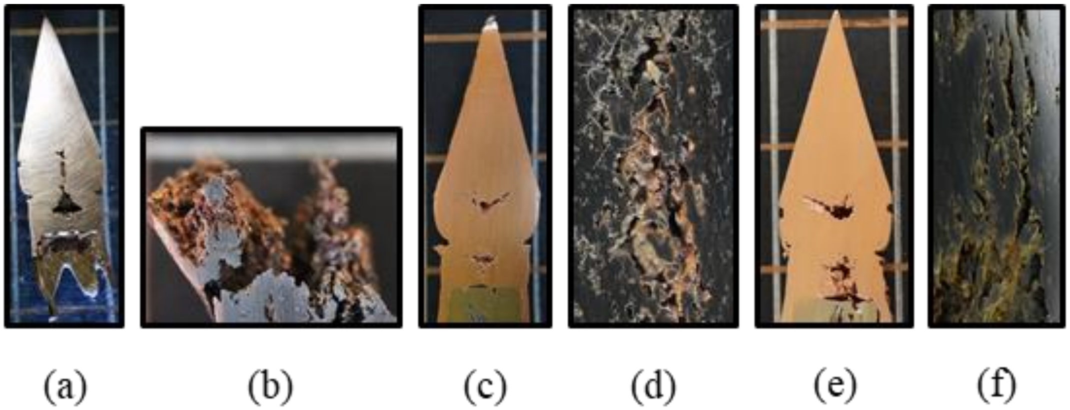

FIGURE 7. Hollow cavity generated in the annulus cone and corresponding copper material deposition in the stainless steel. cores.

CONCLUSION

Understanding how the microstructure fails under explosive compaction can enable system designs that can control the failure process. AM techniques can create hierarchical energy-absorbing and failure regions, integrated into one system. This provides designed anisotropic strength and will enable increased performance while simultaneously reducing the overall system weight. This paper demonstrated how materials created with different AM process parameters failed under explosive compaction along with a traditionally manufactured material. The peak pressure and tensile stress acting on the samples were designed to exceed the strength of the material, so an examination could be conducted on how the material failed under explosively driven dynamic loading. The results presented in this paper illustrate how the microstructures associated with the manufacturing process determines the material failure. Specifically, the melt pool boundaries produced during the AM processing resulted in granular like failure of the material. The layers associated with the cold-rolled stainless steel core resulted in a splintering of the material.

Future work will identify how a lower compressive force acting on the core to identify the initial failure points for each material. Future work will also examine how laser power, scan-speed, hatch spacing, and layer thickness influence the performance of AM cores under a lower compaction force. As well as, explore different AM materials under similar compaction studies as well as ring expansion tests to generate material models for AM process parameters.

REFERENCES

1 Ho J., Lough C., Mulligan P., Kinzel E., Johnson C., Proceedings of the 29th Annual International Solid Freeform Fabrication Symposium – An Additive Manufacturing Conference, 2018.
2 Ho J., Lough C., Mulligan P., Kinzel E., Johnson C., Proceedings of the International Society of Explosive Engineers 45th Annual Conference on Explosives and Blasting Technique, Nashville TN, 2019.
3 Phillip Mulligan, Catherine Johnson, Jason Ho, Cody Lough, and Edward Kinzel, Hypervelocity Impact Symposium, Destin, FL, 2019.
4 R. A. Pruemmer, T. Balakrishna Bhat, K. Siva Kumar, K. Hokamoto, New Hampshire: Science Publishers, 2006.
5 M. Myers, New York: John Wiley & Sons, INC., 1994.
6 L. Chhabildas, L. Davidson, and Y. Horie, New York: Springer, 2005.
7 S. S. Batsanov, New York: Springer-Verlag, 1994.
8 J. Rinehart, J. Pearson, New York: Pergamon Press, 1963.
9 P. W. Cooper, Wiley-VCH, 1996, p. 387.
10 M. A. Cook, Robert E. Krieger Publishing CO. INC., 1958.
11 T. DebRoy, H.L. Wei, J.S. Zuback, T. Mukherjee, J.W. Elmer, J.O. Milewski, A.M. Beese, A. Wilson-Heid, A. De, W. Zhang, Progress in Materials Science, p. 112–224, 2018.